*Invited Paper*

# Multi-frequency notch filters and corrugated 200 to 400 GHz waveguide components manufactured by stacked ring technology

M. Thumm [1*], D. Wagner [2], E. de Rijk [3], W. Bongers [4], W. Kasparek [5], F. Leuterer [2], A. Macor [3], J.-Ph. Ansermet [6], F. Monaco [2], M. Münich [2], H. Schütz [2], J. Stober [2], H. v.d. Brand [4], and A.v. Bieren [3]
[1] Karlsruhe Institute of Technology (KIT), IHM and IHE, Karlsruhe, Germany
[2] Max-Planck-Institut für Plasmaphysik (IPP), EURATOM-IPP, Garching, Germany
[3] SWISSto12 SA, Science Park - EPFL, Lausanne, Switzerland
[4] Dutch Institute for Fundamental Energy Research, EURATOM-DIFFER, Nieuwegein , Netherlands
[5] Institut für Grenzflächenverfahrenstechnik und Plasmatechnologie (IGVP) , Universität Stuttgart, Germany
[6] Laboratoire de Physique des Matériaux Nanostructurés, EPFL, Lausanne, Switzerland
[*1] Email: manfred.thumm@kit.edu

(Received November 30, 2013)

**Abstract**: Sensitive millimeter wave diagnostics need often to be protected against unwanted radiation like, for example, stray radiation from high power Electron Cyclotron Heating applied in nuclear fusion plasmas. A notch filter based on a waveguide Bragg reflector (photonic band-gap) may provide several stop bands of defined width within up to two standard waveguide frequency bands. A Bragg reflector that reflects an incident fundamental $TE_{11}$ into a $TM_{1n}$ mode close to cutoff is combined with two waveguide tapers to fundamental waveguide diameter. Here the fundamental $TE_{11}$ mode is the only propagating mode at both ends of the reflector. The incident $TE_{11}$ mode couples through the taper and is converted to the high order $TM_{1n}$ mode by the Bragg structure at the specific Bragg resonances. The $TM_{1n}$ mode is trapped in the oversized waveguide section by the tapers. Once reflected at the input taper it will be converted back into the $TE_{11}$ mode which then can pass through the taper. Therefore at higher order Bragg resonances, the filter acts as a reflector for the incoming $TE_{11}$ mode. Outside of the Bragg resonances the $TE_{11}$ mode can propagate through the oversized waveguide structure with only very small Ohmic attenuation compared to propagating in a fundamental waveguide. Coupling to other modes is negligible in the non-resonant case due to the small corrugation amplitude (typically $0.05\cdot\lambda_0$, where $\lambda_0$ is the free space wavelength). The Bragg reflector was optimized by mode matching (scattering matrix) simulations and manufactured by SWISSto12 SA, where the required mechanical accuracy of $\pm$ 5 $\mu m$ could be achieved by stacking stainless steel rings, manufactured by micro-machining, in a high precision guiding pipe (patent is pending). The two smooth-wall tapers were fabricated by electroforming. Several measurements were performed using vector network analyzers from Agilent (E8362B), ABmm (MVNA 8-350) and Rohde&Schwarz (ZVA24) together with frequency multipliers. The stop bands around 105 *GHz* (- 55*dB*) and 140 *GHz* (-60*dB*) correspond to the $TE_{11}$-$TM_{12}$ and $TE_{11}$-$TM_{13}$ Bragg resonances. Experiments are in good agreement with theory. The stacked rings technology has also been employed for manufacturing of oversized (I.D. = 15 *mm*) corrugated waveguides (propagating the balanced $HE_{11}$ hybrid mode). The waveguides are for use in a 4 *m* long transmission line for Dynamic Nuclear Polarization Nuclear Magnetic Resonance applications in the 200 to 400 *GHz* band. A high performance flange connection system between the modules allows for modular path building. To validate the performance of the proposed system, a detailed characterization of all corrugated waveguide components has been performed using a Vector Network Analyzer operating in the 220 to 330 *GHz* range.

**Keywords**: Electron cyclotron heating, Gyrotrons, Plasma diagnostics, Bragg reflector notch filter, Dynamic nuclear polarization, Oversized Terahertz $HE_{11}$-mode transmission line, Stacked rings manufacturing technology

**doi:** 10.11906/TST.212-222.2013.12.15

## 1. Introduction

Sensitive millimeter wave diagnostics are vulnerable to stray radiation from gyrotrons applied in Electron Cyclotron Resonance Heating (ECRH) systems at thermonuclear fusion plasma experiments. The output power of modern high-power fusion gyrotrons is typically in the megawatt range with pulse lengths from several seconds to continuous wave (CW). This means that even a small fraction of the total injected power has the potential to destroy sensitive millimeter wave diagnostic receivers. The stray radiation can originate from non-perfect coupling to the plasma (e.g. wrong polarization of the injected millimeter wave beam) or reflections at plasma density cutoffs. There are also heating schemes at harmonics of the electron cyclotron frequency with incomplete absorption of the injected millimeter wave power. For modern ECRH systems using multi-frequency or frequency step-tunable gyrotrons, filters with more than one stop-band are required. At the same time the stop band must be rather wide (several hundreds of MHz) in order to cope for the gyrotron frequency chirp, especially at the beginning of the pulse when the cavity expands due to Ohmic losses and the electron cyclotron frequency changes due to neutralization of the electron beam by residual ions. The stop band must also include slightly different oscillating frequencies in systems using more than one gyrotron. Both requirements are difficult to fulfill using the available filter technology (coupled cavity filters or quasi-optical resonance filters) [1]. A filter based on an oversized circular corrugated waveguide with a corrugation period satisfying the Bragg condition can provide several defined stop bands with steep frequency slopes and well defined width. Such a filter was successfully built and tested in Ka-Band [2]. We applied the same design principle for a filter which will protect a new inline Electron Cyclotron Emission (ECE) diagnostic at ASDEX Upgrade [3] where a multi-frequency ECRH system with several two-frequency gyrotrons (105 and 140 *GHz*) is in operation. The Bragg reflector was optimized by mode matching (scattering matrix) simulations and manufactured by SWISSto12 SA, where the required mechanical accuracy of $\pm$ 5 $\mu m$ could be achieved by stacking stainless steel rings, manufactured by micro-machining, in a high precision guiding pipe (patent is pending) [4].

The stacked rings technology has also been employed for manufacturing of oversized (I.D. = 15 *mm*) corrugated waveguides, propagating the balanced $HE_{11}$ hybrid mode. The waveguides are for use in a 4 *m* long transmission line for Dynamic Nuclear Polarization (DNP) Nuclear Magnetic Resonance applications (NMR) in the frequency range of 200 to 400 *GHz*. The novel components are designed to enable broadband and low loss propagation. By employing high precision manufacturing, this novel technology extends the frequency range accessible by corrugated $HE_{11}$-mode waveguide components to 400 *GHz* and beyond. This opens the way for better performance in applications such as DNP and gas spectroscopy, magnetic resonance techniques or near field probe measurements using sub-THz waves. These waveguides have an excellent broadband behavior and an efficient coupling to the $TEM_{00}$ fundamental Gaussian mode for free space propagation.

## 2. Notch filter principle

The principle scheme of the notch filter is sketched in Figs.1 and 2. A Bragg reflector that reflects an incident circular waveguide $TE_{11}$ mode into a $TM_{1n}$ mode close to cutoff is combined with two non-linear waveguide tapers to fundamental waveguide diameter. Here the fundamental $TE_{11}$ mode is the only propagating mode at both ends of the reflector. The incident $TE_{11}$ mode propagates through the taper and is converted to the high order $TM_{1n}$ mode by the Bragg structure at the specific Bragg resonances (Fig. 2). The $TM_{1n}$ mode is trapped in the oversized waveguide section by the tapers. Once reflected at the input taper, it will be converted back into the $TE_{11}$ mode which then can pass through the taper. Therefore at higher order Bragg resonances, the filter acts as a reflector for the incoming $TE_{11}$ mode. Outside of the Bragg resonances the $TE_{11}$ mode can propagate through the oversized waveguide structure with only very small Ohmic attenuation compared to propagating in a fundamental waveguide. Coupling to other modes is negligible in the non-resonant case due to the small corrugation amplitude (typically $0.05 \cdot \lambda_0$, where $\lambda_0$ is the free space wavelength).

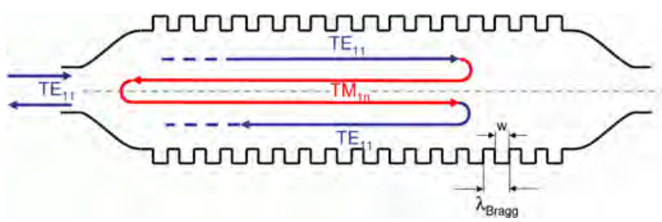


Fig. 1 Principle scheme of the notch filter employing higher order Bragg resonances.

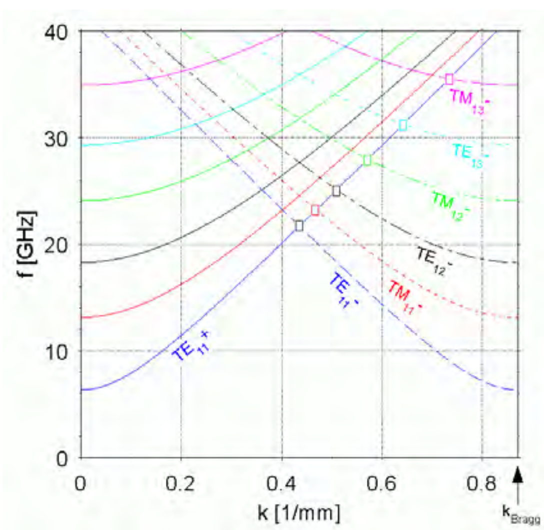


$$\lambda_{Bragg} = \frac{2\pi}{k_{Bragg}} = \frac{2\pi}{k_{z1} + k_{z2}}$$

Fig. 2 Dispersion diagram of higher order Bragg resonances. Incident modes are marked with '+' whereas reflected modes are tagged with '-'.

## 3. Notch filter design

The Bragg reflector has a tapered corrugation profile at both ends (Fig. 3) to ensure high mode purity and minimum side bands in the frequency response [2]. The corrugation amplitude profile is given by:

$$h(z) = h_0 \cdot \frac{\sin\left(\pi \cdot \left(1 - \frac{z}{z_0}\right)\right)}{\pi \cdot \left(1 - \frac{z}{z_0}\right)} \tag{1}$$

where $h_0$ is the maximum corrugation amplitude and $z_0$ is the total length of the tapered section of the corrugation.

The corrugations in the middle section of the Bragg reflector have a constant depth of $h_0$. To provide two stop bands at 105 and 140 *GHz*, the required waveguide radius is 3.47 *mm* (Fig. 4). The total number of Bragg corrugation periods is 250, where each period is 2.1 *mm* long. The design goal was to provide two stop bands, each with a width of ~800 *MHz* and a suppression of around 50-60 *dB* at the center frequencies of 104.75 and 139.75 *GHz*. The geometry of the complete filter, including optimized nonlinear tapers to fundamental waveguide at both ends is plotted in Fig. 3.

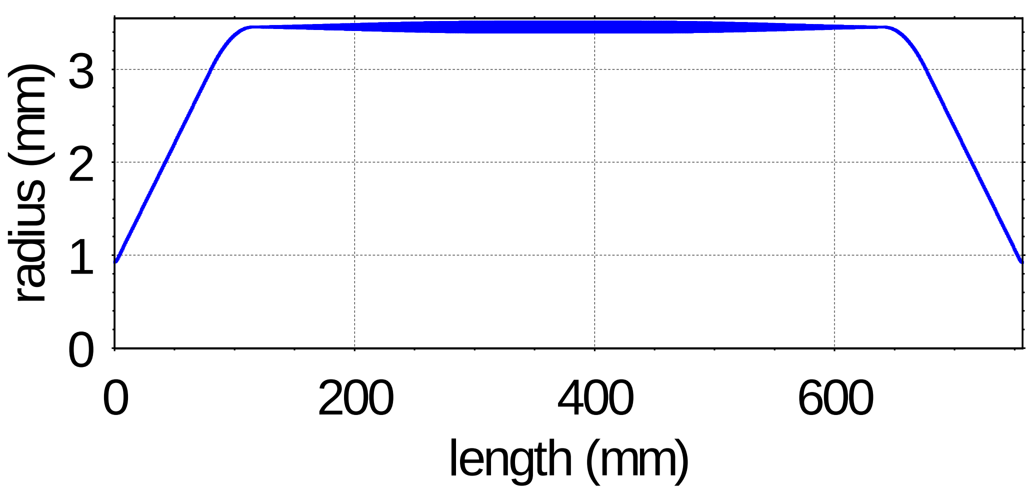


Fig. 3 Bragg reflector with tapered corrugation depth and non-linear waveguide radius tapers at both ends.

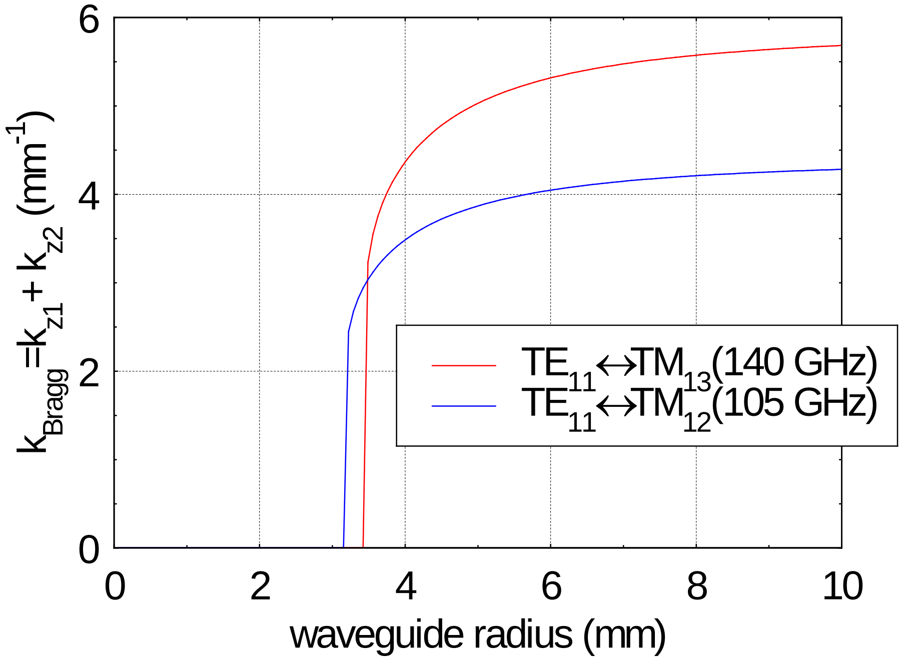


Fig. 4 Determination of the waveguide radius required for the 2-frequency notch filter.

## 4. Experimental results

The corrugated waveguide of the Bragg reflector was manufactured by SWISSto12 SA, where the required mechanical accuracy of ± 5 $\mu m$ could be achieved by stacking stainless steel rings, cut by electric discharge machining, in a high precision guiding pipe (Fig. 5) [4]. The two smooth-wall non-linear tapers were fabricated by copper electroforming. The tapers are connected to the oversized Bragg reflector by collar flanges (Fig. 6). Additionally circular to rectangular standard waveguide transitions are connected to the smooth-wall tapers at both ends.

Fig. 7 shows calculated and measured transmission of the filter over the full D-Band. The stop bands around 105 and 140 *GHz* correspond to the $TE_{11}$-$TM_{12}$ and $TE_{11}$-$TM_{13}$ Bragg resonances. The suppression at the $TE_{11}$-$TE_{13}$ and $TE_{11}$-$TE_{14}$ resonances at 121 and 162 *GHz* is much less due to the low coupling of TE modes at the corrugations. Figs. 8 and 9 show measurements of the stop bands around 105 and 140 *GHz*. The measurements were performed with different setups: Agilent Vector Network Analyzer E8362B, Rohde&Schwarz Vector Network Analyzer ZVA24 and ABmm Vector Network Analyzer MVNA 8-350 with frequency multipliers. The measurements were probably somewhat limited by the spectral purity of the output signals. However, both center frequencies and stop band widths are in good agreement with the calculated values, proving a very high mechanical accuracy of the Bragg reflector. The suppression inside of the notch is somewhat less than theoretically predicted, but still shows a good performance of the filter. Further optimization is possible e.g. by avoiding parasitic reflections at waveguide flanges.

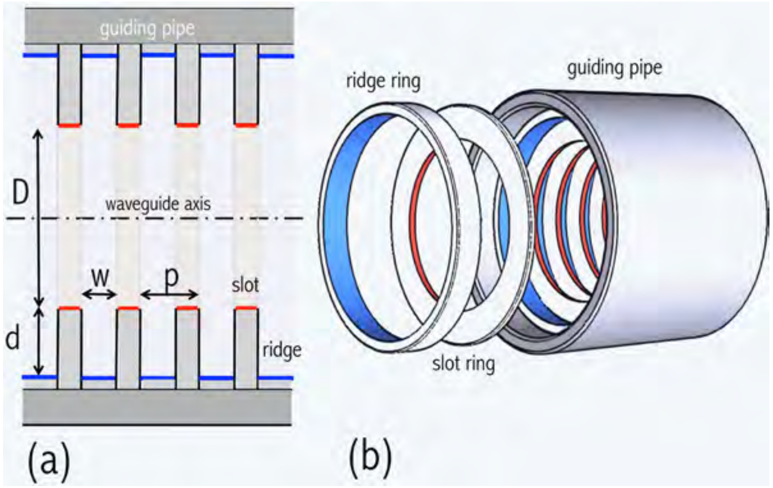


Fig. 5 Corrugated waveguide made from stacked rings. (a) Schematic view of a corrugated waveguide with inner diameter D, corrugation period p, slot width w and slot depth d. (b) The corrugation is obtained by alternatingly piling up slot and ridge rings into a guiding pipe [4].

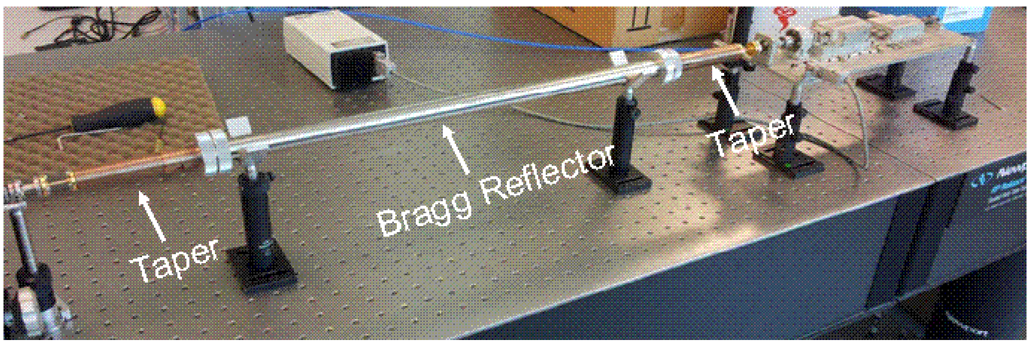


Fig. 6 Multi-frequency notch filter setup with Bragg reflector and up-and down-tapers.

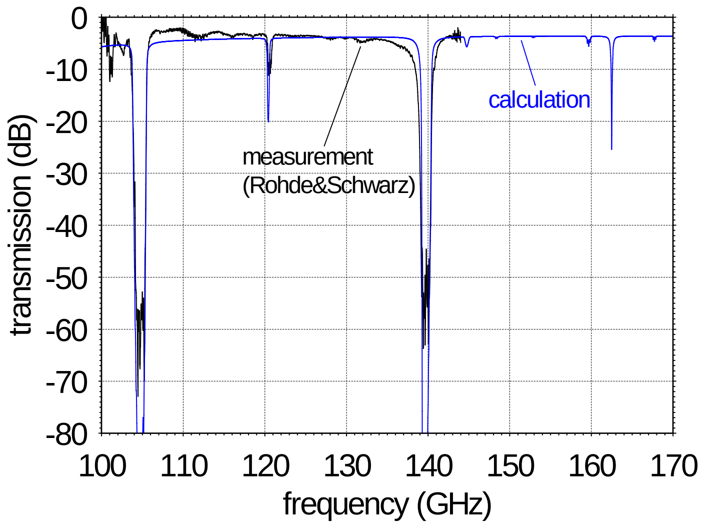


Fig. 7 Calculated and measured transmission of the multi-frequency notch filter. Calculations were done using the mode matching method (scattering matrix calculations). Measurements were performed with the Rohde&Schwarz Vector Network Analyzer (ZVA24).

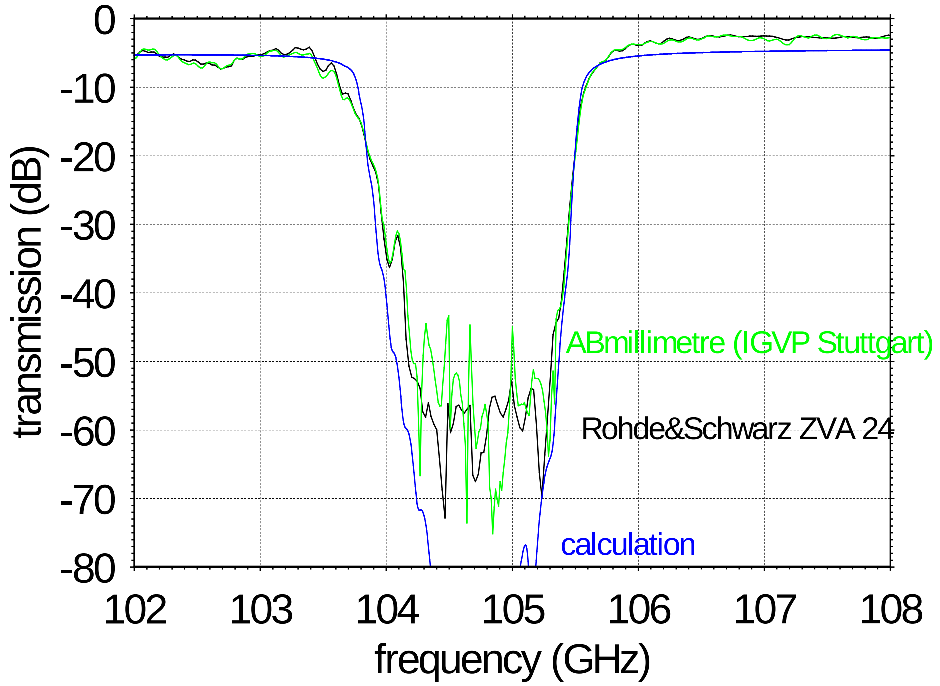


Fig. 8 Comparison between calculated and measured transmission around 105 *GHz*.

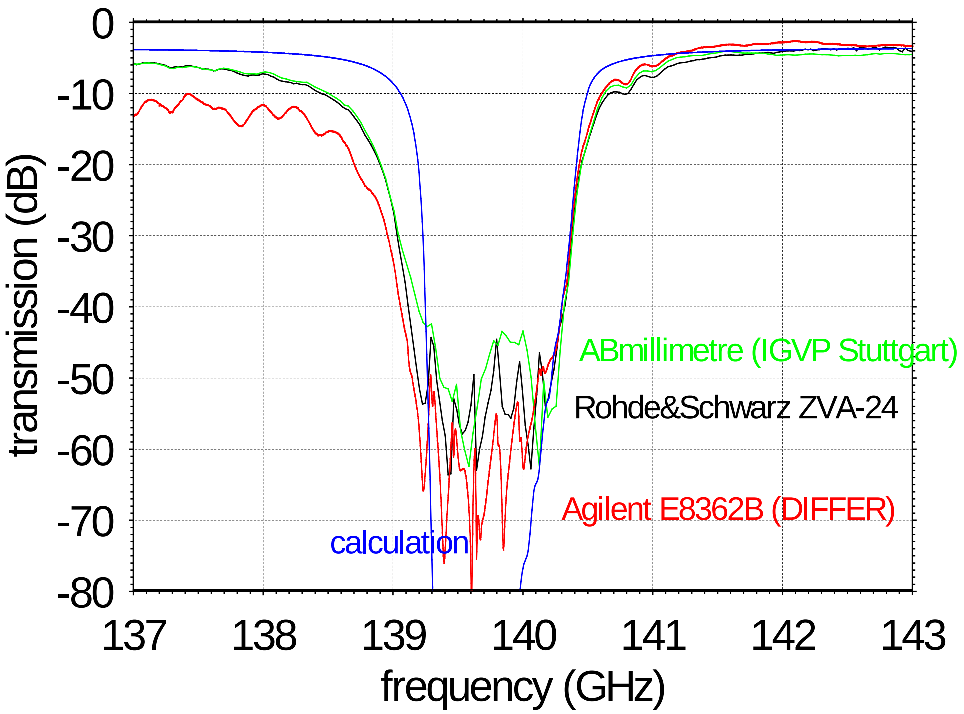


Fig. 9 Comparison between calculated and measured transmission around 140 *GHz*.

## 5. Oversized 200 to 400 *GHz* corrugated $HE_{11}$-mode waveguide

A set of corrugated waveguide modules for the balanced $HE_{11}$-hybrid mode [5] has been manufactured by SWISSto12 SA employing their stacked rings technology. The waveguide modules have an inner diameter of 15 *mm* and a length of 500 *mm*. They are assembled with a precise flange connection system. The losses of this overmoded waveguide have been computed based on theoretical losses for these structures [6], and are plotted in Fig. 10.

These low-loss waveguide components are for use in Terahertz Dynamic Nuclear Polarization Nuclear Magnetic Resonance (DNP-NMR) experiments. In this spectroscopy technique, NMR is performed simultaneously with Electron Spin Resonance (ESR) in free radical molecules. This dual approach enables a substantial increase in the achievable signal to noise ratio of the NMR measurements. The corrugated $HE_{11}$ waveguides are used to build a 4 *m* long transmission line between a DNP-NMR spectrometer and a gyrotron oscillator source operating at 263 *GHz*.

To validate the performance of the proposed system, a detailed characterization of all corrugated waveguide components has been performed using a Vector Network Analyzer operating in the WR-3.4 band (220 to 330 *GHz*) with frequency extension modules (see Fig. 11).

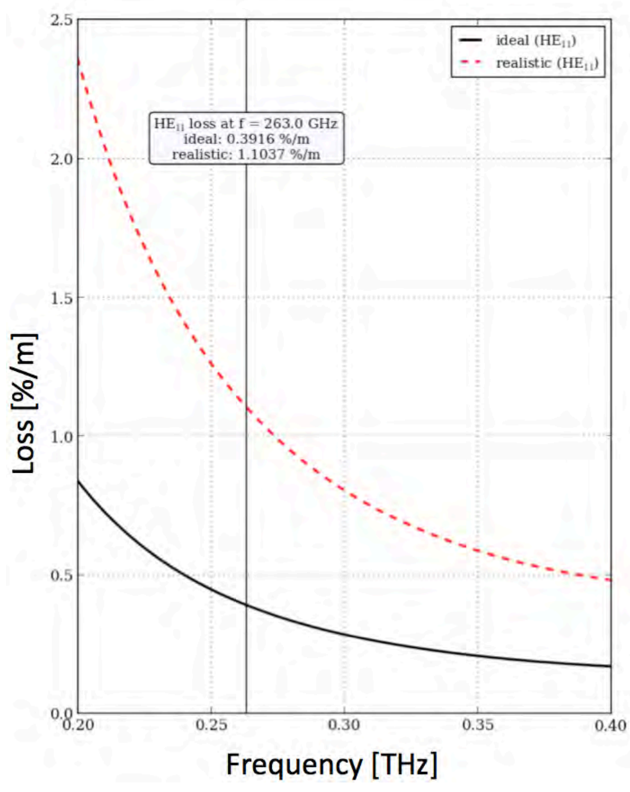


Fig. 10 Modeled theoretical power losses for the $HE_{11}$ mode propagating through the corrugated waveguides manufactured for this study. The black solid curve represents the losses assuming the conductivity of bulk Titanium. The red dashed curve show a realistic model for losses, which assumes half the conductivity of bulk Titanium. This safety factor is used to compensate for imperfections in the material and surface roughness effects.

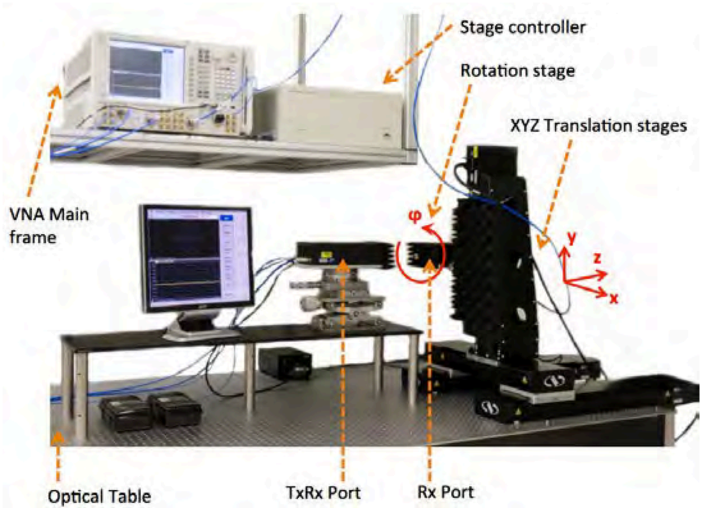


Fig. 11 Photograph of the Vector Network Analyzer (VNA) test bench. The VNA main frame is linked to frequency extension modules capable of Transceiving (TxRx) or Receiving (Rx). The Receiver is mounted on an XYZ translation stage to measure field cartographies. A rotation stage enables measurements of different beam polarizations. The test bench is based on an optical table platform.

The sub-THz beam at the output of the transceiving frequency extension module of the VNA is launched into free space by a corrugated horn antenna. This quasi-Gaussian beam is re-focalized by a dielectric lens to couple efficiently to the $HE_{11}$ mode inside the overmoded corrugated waveguide. Results of the field cartography measurements performed at the input and the output of the corrugated waveguide are shown in Fig. 12.

Based on the measured field cartographies at the output aperture of the corrugated waveguide, the $HE_{11}$ mode content propagated through the waveguide can be determined [7], see Fig 13.

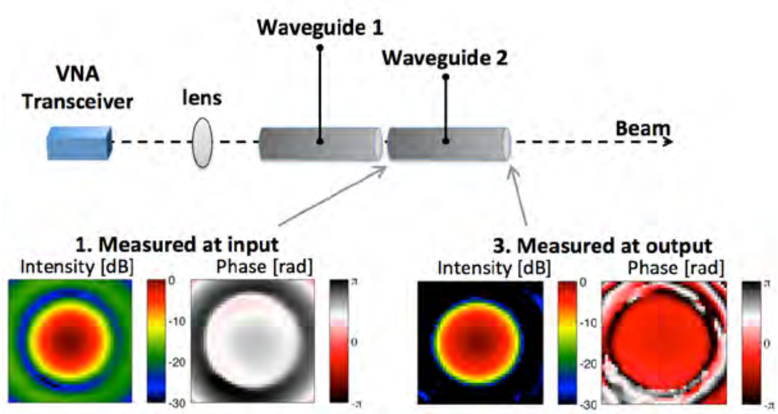


Fig. 12 Block diagram of the experimental setup (Top). The sub-THz beam is generated by a VNA transceiver and launched into free space by a corrugated horn antenna. This quasi-Gaussian beam is re-focalized by a dielectric lens to optimize the coupling to the $HE_{11}$ beam inside a first corrugated waveguide module (length = 500 *mm*). Further corrugated waveguide modules can be connected to the first one by precision flanges. (Bottom Left) Measured beam intensity profiles at the output of the first corrugated waveguide module (coinciding with the input of the second module). (Bottom Right) Measured beam profile at the output of the second corrugated waveguide module. Both beams shows a high $HE_{11}$ mode purity, which confirms that the waveguide propagates the low loss $HE_{11}$ mode.

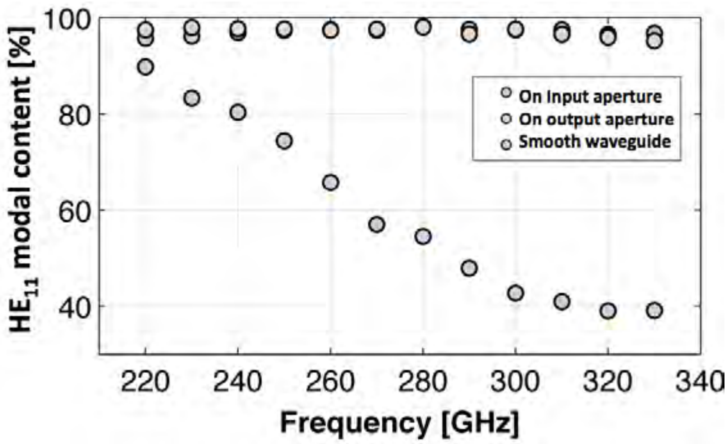


Fig. 13 $HE_{11}$ Mode content measured at the input and output aperture of a corrugated waveguide excited with the $HE_{11}$ mode. Measurements are shown as a function of the propagated signal frequency. For comparison, the measured mode-content at the output aperture of a cylindrical smooth waveguide is shown. This cylindrical smooth waveguide is excited by a high purity $HE_{11}$ mode at its input.

## 6. Conclusions

Two-frequency Bragg reflector waveguide notch filters (105 and 140 *GHz*) for suppression of gyrotron RF stray radiation in nuclear fusion plasma diagnostics experiments (ASDEX Upgrade and Wendelstein 7-X in Germany) during ECRH with high power gyrotrons have been manufactured with high precision using the stacked rings technology. The filters show low insertion loss, steep frequency slopes and wide stop band. The center frequencies are in good agreement with theory. Further optimization can be achieved by improving/avoiding the waveguide flanges.

The stacked rings technology has also been employed for the production of a set of corrugated waveguide modules for the balanced $HE_{11}$-hybrid mode (inner diameter = 15 *mm*, module length = 500 *mm*). The waveguides are tested on a Vector Network Analyzer setup between 220 and 330 *GHz* and show the propagation of the $HE_{11}$ mode with a mode purity above 95% across the whole frequency band. Commercial versions of these waveguide components manufactured by SWISSto12 SA are available over a set of frequency bands.

## References

[1] P. Woskov. "Notch filter options for ITER stray gyrotron radiation". *Proc. 13$^{th}$ International Symposium on Laser Aided Plasma Diagnostics*, Takayama, Japan (2007).

[2] D. Wagner, W. Kasparek, F. Leuterer, et al.. "Bragg reflection band stop filter for ECE on Wega". *J. Infrared Milli Terahz Waves*, 32, 1424–1433 (2011).

[3] W.A. Bongers, W. Kasparek, N. Doelman, et al.. “Commissioning of inline ECE system within waveguide based ECRH transmission systems on ASDEX upgrade”. *EPJ Web of Conferences*, 32, 03006 (2012)

[4] E. de Rijk, A. Macor, J.-P. Hogge, et al.. “Note: Stacked rings for Terahertz wave-guiding”. *Rev. Sci. Instruments* 82, 066102 (2011).

[5] M.K. Thumm, W. Kasparek. “Passive high-power microwave components”. *IEEE Trans. on Plasma Science,* 30, 755-786 (2002).

[6] J.L. Doane. “Propagation and mode coupling in corrugated and smooth-wall circular waveguides”. *Infrared and Millimeter Waves (Academic Press, Inc. Orlando, FL),* 13 (1985).

[7] H. Idei, M. Shapiro, R.J. Temkin, et al.. “Mode content analysis in circular corrugated waveguide using radiated field”. *Proc. Joint 32nd International Conference on Infrared and Millimeter Waves and 15th International Conference on Terahertz Electronics (IRMMW-THz 2007),* Cardiff, UK, 69–70 (2007).

[8] S.K. Jawla, E.A. Nanni, M.A. Shapiro, et al.. “Mode content determination of Terahertz corrugated waveguides using experimentally measured radiated field patterns”. *IEEE Trans. on Plasma Science*, 40, 1530-1537 (2012).